

Use of YB₆₆ as monochromator crystals for soft-energy EXAFS

A. D. Smith,^{a*} B. C. Cowie,^a G. Sankar^b and J. M. Thomas^b

^aDaresbury Laboratory, Central Laboratories to the Research Councils, Warrington, Cheshire WA4 4AD, UK, and ^bThe Royal Institution of Great Britain, 21 Albemarle Street, London W1X 4BS, UK. E-mail: a.d.smith@dl.ac.uk

(Received 4 August 1997; accepted 15 December 1997)

YB₆₆(400) crystals present a new advance in monochromator crystals suitable for use at energies below 2 keV. In this paper a comparison of their performance with that provided by the more usual beryl and quartz crystals, which cover the same energy range, is presented. In general, the YB₆₆ crystals are much superior; however, they do exhibit a pair of large 'crystal glitch'-type features in the 1380–1440 eV region. These fall in the Mg *K*-EXAFS region and so can present a serious problem in studies of this edge for a wide range of materials. An important class of materials so afflicted are magnesium-substituted aluminophosphate molecular sieves (zeolites), which are used in many applications, in particular as solid acid catalysts for conversion of methanol to hydrocarbon.

Keywords: monochromators; YB₆₆; aluminophosphate; magnesium.

1. Introduction

To provide monochromatic X-ray beams in the soft X-ray energy range (1–4 keV) it is necessary to use a variety of monochromator crystals with different *2d* spacings. Above about 1700 eV, semiconductor crystals such as InSb(111), Ge(111) and Si(111) with *2d* spacings of 7.48 Å and below can be used. Due to their semiconducting nature, these are thermally robust and can happily endure long exposure to the intense beams of X-rays available from synchrotron sources. Below this energy lie the aluminium and magnesium *K*-absorption edges (1559 and 1303 eV, respectively). In the past it has been necessary to use quartz and beryl crystals to access these two edges. However, these crystals are very susceptible to radiation damage with significant degradation in performance (throughput and rocking-curve widths) occurring within days of use.

In recent years Rowen *et al.* (1993) and Wong *et al.* (1994) have reported good results with an artificial crystal, YB₆₆(400). However, the manufacturing process is complex and the crystals remained unavailable to the general synchrotron radiation community for several years after the first publication of results. Some of the fabrication difficulties have now been overcome and the crystals are now available commercially from Crystal Systems Inc., Japan.

The YB₆₆ crystal structure has a face-centred cubic structure with a unit-cell dimension of 23.52 Å. The crystals are cut on the (400) plane which has the strongest reflection and gives a *2d* spacing of 11.76 Å. Due to the semiconducting nature of the

crystals, they have good thermal stability and exhibit a resilience to synchrotron radiation. The *2d* spacing gives these crystals a useful energy range from 1071 to 6071 eV. This is not quite sufficient to allow proper coverage of the sodium *K*-edge at 1070 eV, bearing in mind the need to encompass a pre-edge region of some 20 to 30 eV for EXAFS analysis. Nevertheless, the ability to cover in principle the Mg, Al and Si *K*-edges with a single pair of monochromator crystals is attractive as many zeolite materials contain all three elements. This is an important class of material due to their many commercial applications (such as supports for exhaust catalysts, washing powders *etc.*) and previously required the use of separate monochromator crystals for each edge [beryl, quartz and InSb(111)].

2. Measured performance of YB₆₆

Tests on BL3.4 at the SRS (MacDowell *et al.*, 1988; Roper *et al.*, 1992) permit a comparison to be made between YB₆₆, beryl and quartz monochromator crystals. The effective reflectivity of the crystals was determined by using the drain current from a 0.75 µm aluminium foil to measure the monochromator output flux. A comparison between YB₆₆ at 1250 eV with routine measurements for newly cut and polished beryl crystals taken at 1300 eV give values of 0.9×10^{-11} A and 0.3×10^{-10} A per 100 mA stored SRS current, respectively. However, the flux obtained from beryl falls with time to less than 0.7×10^{-11} A per 100 mA after approximately 500 h use. More problematically, the double-crystal rocking curves (DCRC) for beryl broaden significantly and often become double- rather than single-peaked. The recorded DCRC widths increase from 0.9 eV FWHM to over 3.0 eV FWHM, as opposed to a consistent 0.4 eV for YB₆₆. DCRC widths are useful indicators of the energy resolution of the crystals. YB₆₆ crystals, like other semiconductor crystals, do not exhibit any degradation in performance over this time period.

A comparison at 1500 eV between YB₆₆ and quartz gives throughputs of 0.8×10^{-11} A and 1.5×10^{-11} A per 100 mA, respectively. However, quartz crystals degrade quickly and this last figure drops to less than 0.4×10^{-12} A per 100 mA over 100 h or so exposure to beam. DCRC widths for quartz similarly degrade from 0.3 eV FWHM to >2 eV FWHM; for YB₆₆ this figure stays at 0.6 eV FWHM.

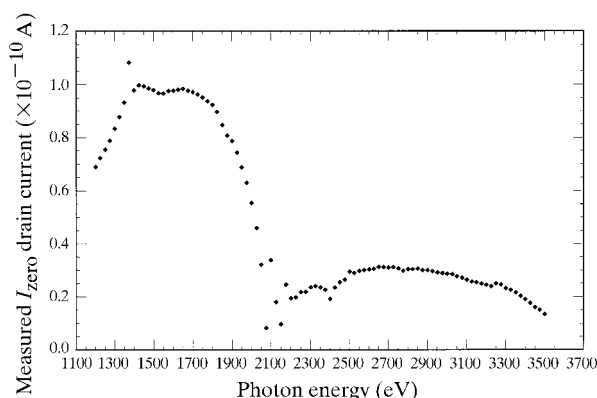


Figure 1 The spectral response from YB₆₆ monochromator crystals on BL3.4. The beamline optics are set to give a high-energy cutoff at about 3500 eV.

Beamline BL3.4 is equipped with a planar first mirror with an adjustable angle of incidence. In addition, it can be translated to present one of two coatings, either 500 Å chromium or a dual layer of 1250 Å carbon on 3500 Å silicon to the X-ray beam. This allows the high-energy cutoff of the beamline to be easily altered to reduce the power loading for the thermally sensitive beryl and quartz crystals. A second toroidal focusing mirror is positioned such that light from the pre-mirror always strikes it at a constant angle of incidence, thereby ensuring that the focus condition through the monochromator and onto the sample remains the same. The measurements for these crystals were made using beamline characteristics relevant for them; therefore their reflectivities cannot be compared directly with that for YB₆₆, rather they provide a measure of the flux obtainable under realistic operating conditions.

The spectral response of the YB₆₆ monochromator crystals over the energy range 1100–3500 eV is shown in Fig. 1. The sharp cutoff at approximately 2000 eV can be attributed to the occurrence of the yttrium *L*-edges at 2080, 2156 and 2373 eV, which restrict the useful range of the crystals and would limit Si *K*-EXAFS scans to $k = 8$. This is not a severe problem as the silicon *K*-range is better covered by InSb(111) crystals which have a significantly higher throughput; a flux of 0.5×10^{-9} A per 100 mA stored beam being recorded at an energy of 2000 eV for InSb(111) as opposed to 0.6×10^{-11} A for the

YB₆₆. The DCRC widths remain comparable at 1.6 eV FWHM and 1.4 eV FWHM, respectively.

Their low reflectivity compared with crystals such as InSb(111) makes YB₆₆ unsuitable for the low signal levels encountered in surface EXAFS experiments; however, it is sufficient for bulk EXAFS studies.

In the energy range ~1400 eV there are two pronounced features, one at about 1385 eV, which is evident in Fig. 1. A second slightly lower intensity feature also exists at about 1437 eV. These are of concern as they lie in the Mg *K*-EXAFS region. Their presence can be determined to arise from a spurious reflection off the (600) plane at Bragg angles which correspond to the energy of the yttrium *L*-absorption edges (Tanaka *et al.*, 1997). At these energies the atomic scattering factors for yttrium change enormously and allow the low-concentration yttrium to interact much more strongly with the incident X-ray flux. These spurious higher-order reflections only cause problems with samples which contain elements with absorption edges between them and the lower primary radiation. This presents a potentially serious problem for Mg *K*-EXAFS analysis.

There are two possible solutions to this problem. The first is to use an energy-discriminating fluorescence detector such as a solid-state detector (Smith *et al.*, 1995) to pick out the Mg *K α* fluorescence line from the other conflicting ones. The second uses the adjustable high-energy cutoff of beamline BL3.4 to reduce the flux above 2000 eV and hence prevent the yttrium reflections occurring in the first place. Fig. 2 shows the change in throughput as a function of the M1 incidence angle for the dual C/Si coating, and the effect this has on the Y *L*_{2,3} features can be seen in Fig. 3.

In practice we have determined that due to the strength of these spurious Y *L*_{2,3} structures it is often necessary to combine both these techniques, especially for many of the magnesium-substituted aluminosilicate/phosphate class of materials.

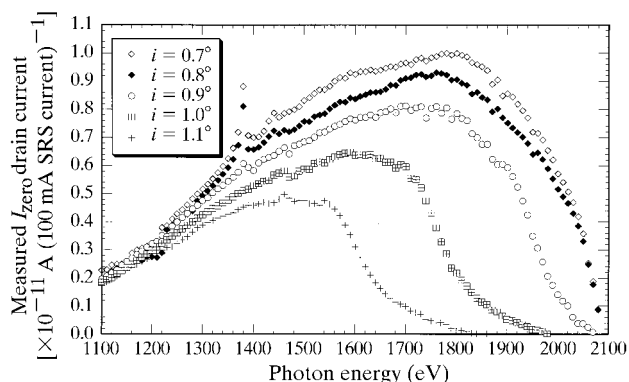


Figure 2
Reduction of the high-energy cutoff of beamline BL3.4 achieved by increasing the angle of incidence on the carbon/silicon-coated pre-mirror (M1).

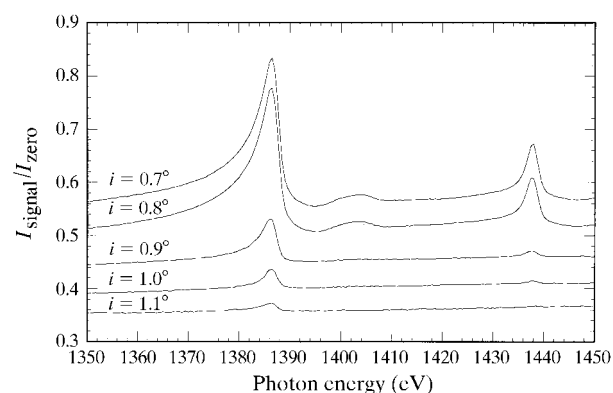


Figure 3
Effect of reducing the cutoff energy on the strength of the 'glitches'. All plots are to the same vertical scale, but displaced by 0.05 for clarity.

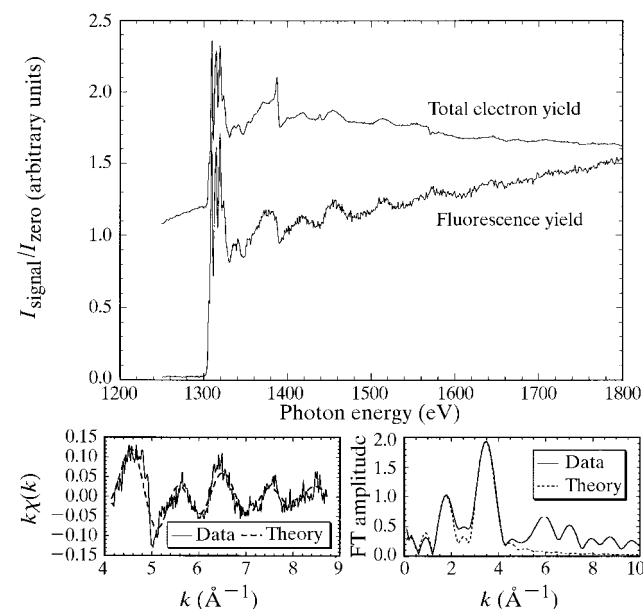


Figure 4
Total electron and fluorescent Mg *K*-EXAFS spectra of MgCr₂O₄ with analysis, collected simultaneously using YB₆₆ crystals and a beamline cutoff of 2000 eV.

We have also noted the presence of genuine second-order harmonic content, passage of this being permitted by the (400) reflection from the cubic structure of the YB₆₆.

3. Magnesium-substituted aluminium and gallium phosphates

There is considerable interest in the field of manufacturing microporous materials. Cobalt-substituted gallophosphate (CoGaPO) is one such system (Overweg *et al.*, 1998; Wright *et al.*, 1993; Chen & Thomas, 1993). However, the loss of structural integrity at elevated temperatures (above 573 K) limits its potential application as a catalyst. Work at the Royal Institution is taking place to see whether this limit can be increased by substituting other divalent metal ions such as Mg²⁺, Fe²⁺ and Zn²⁺ for the cobalt. Similarly, Mg²⁺-substituted aluminophosphates, such as Mg-DAF1 and MgAlPO-18, make good solid acid catalysts. To derive local structural information around the Mg ions it is necessary to obtain good quality Mg *K*-edge data for these materials and suitable model compounds. One such model system is MgCr₂O₄ wherein Mg²⁺ ions occupy tetrahedral sites.

Fig. 4 demonstrates the quality of EXAFS data obtained from this system using the solid-state detector in conjunction with a suitably selected high-energy cutoff with YB₆₆ crystals in the BL3.4 monochromator. A comparison between total electron yield and fluorescence methods shows the benefit of energy-

resolving fluorescence detection in combination with tuned cutoff optics to remove the effects of the yttrium *L*-edge features in the Mg *K*-edge EXAFS region. The $\chi(k)$ and Fourier transform data in Fig. 4 are obtained from the fluorescence data shown in the same figure.

References

- Chen, J. S. & Thomas, J. M. (1993). *J. Chem. Soc. Chem. Commun.* **5**, 603–604.
- MacDowell, A. A., West, J. B., Greaves, G. N. & van der Laan, G. (1988). *Rev. Sci. Instrum.* **59**, 843–852.
- Overweg, A., Sankar, G., Thomas, J. M. & van Santen, R. A. (1998). In preparation.
- Roper, M. D., Buksh, P. A., Kirkman, I. W., van der Laan, G., Padmore, H. A. & Smith, A. D. (1992). *Rev. Sci. Instrum.* **63**(1), 1322–1325.
- Rowen, M., Rek, Z. U., Wong, J., Tanaka, T., George, G. N., Pickering, I. J., Via, G. H. & Brown, G. E. (1993). *Synchrotron Rad. News*, **6**, 25–27.
- Smith, A. D., Derbyshire, G. E., Farrow, R. C., Sery, A., Raudorf, T. W. & Martini, M. (1995). *Rev. Sci. Instrum.* **66**(2), 2333–2335.
- Tanaka, T., Aizawa, T., Rowen, M., Rek, Z. U., Kitajima, Y., Higashi, I., Wong, J. & Ishizawa, Y. (1997). *J. Appl. Cryst.* **30**, 87–91.
- Wong, J., George, G. N., Pickering, I. J., Rek, Z. U., Rowen, M., Tanaka, T., Via, G. H., DeVries, B., Vaughan, D. E. W. & Brown, G. E. (1994). *Solid State Commun.* **92**, 559–562.
- Wright, P. A., Jones, R. H., Natarajan, S., Bell, R. G., Chen, J. S., Hursthouse, M. B. & Thomas, J. M. (1993). *J. Chem. Soc. Chem. Commun.* **7**, 633–635.